

DESIGN AND DEVELOPMENT OF SOLID LIPID NANOPARTICLES CONTAINING ROSUVASTATIN USING CENTRAL COMPOSITE DESIGN

DISHARI DUTTA¹, PRANABESH CHAKRABORTY², CHOWDHURY MOBASWAR HOSSAIN^{3*}

¹Bengal School of Technology, WB, India. ²Department of Pharmaceutical Technology, Maulana Abul Kalam Azad University of Technology, Haringhata-741249 India

*Corresponding author: Chowdhury Mobaswar Hossain; *Email: drcmhossain@gmail.com

Received: 15 Aug 2024, Revised and Accepted: 25 Oct 2024

ABSTRACT

Objective: Rosuvastatin calcium, a BCS class II drug with low solubility, was optimized using a central composite design to improve its bioavailability.

Methods: The study utilized Kolliphor RH 40 as an emulsifier and glyceryl monostearate as a solid lipid in preparing solid lipid nanoparticle dispersion, optimizing formulations based on mean dissolution time and entrapment efficiency.

Results: The study analyzed the entrapment efficiency and mean dissolution time of the prepared solid lipid nanoparticles. The range of mean dissolution time was found 7.1±0.5 to 8.9±0.6 h. The highest entrapment efficiency was found to be 90.28%, with a standard deviation of 0.2. The linear model was chosen based on data precision and trend, while the quadratic model was selected for mean dissolution time. The 3D view graph indicated the model/equation followed by the formulations. The optimized formulation had a particle size of 16.16±10 nm and particle size distribution index to 0.729±0.02, indicating high homogeneity. Transmission electron microscopy images and dynamic light scattering data were in correlation. XRD, DSC used to analyze the drug's transformation into amorphous form. The dissolution profile of different formulations was plotted, and the optimized formulation followed the Korsmeyer-Peppas model. FTIR showed drug peaks, indicating no interaction.

Conclusion: The study suggested that the bioavailability of rosuvastatin calcium can be enhanced through the preparation of solid lipid nanoparticles of smaller size and sustained release of rosuvastatin.

Keywords: Rosuvastatin calcium, Central composite design, Solid lipid nanoparticle, emulsifier, Lipid

© 2025 The Authors. Published by Innovare Academic Sciences Pvt Ltd. This is an open access article under the CC BY license (<https://creativecommons.org/licenses/by/4.0/>) DOI: <https://dx.doi.org/10.22159/ijap.2025v17i1.52360> Journal homepage: <https://innovareacademics.in/journals/index.php/ijap>

INTRODUCTION

Nanoparticles are an appealing delivery mechanism to regulate drug release. Drugs with poor solubility can also be encapsulated/solubilized using solid lipids or liquid lipids [1-3]. Solid lipid nanoparticles (SLNs) are colloidal carrier systems with a solid physiological lipid core that is coated in surfactants and high melting point lipid(s) to lower toxicity risk [4-6]. SLN is attractive and improves the efficacy of medications, nutraceuticals, and other materials because of its unique properties, which include small size, large surface area, high drug loading, entrapment efficiency, and phase interaction at the interface [7, 8].

Solid lipid nanoparticles are useful in solving problems like low solubility and enhance bioavailability. Rai *et al.* 2021 [9] optimized Glyceryl Monostearate based Solid Lipid Nanoparticles of Docetaxel(DTX), the optimal dimension of 100 nm has been shown by optimized DTX-SLNs, accompanied by a low polydispersity index and excellent entrapment efficiency. Glyceryl monostearate is also proven to have good stability and does not show polymorphic changes during storage [10, 11]. Salmerón *et al.* 2023 reported that Kolliphor RH 40 in drug micellar solution of a solid dispersion formulation promotes the presence of micelles that achieve delayed recrystallization [12]. Yasir *et al.* studied the efficiency of SLN in targeting the brain through the nose. The study concluded that the drug can be successfully delivered to the brain via nose by formulating Solid lipid nanoparticles using Compritol 888 ATO as lipid and a combination of Tween 80 and Poloxamer188 as emulsifiers [13]. A current study shows that melatonin-loaded SLN had better neuroprotective effects in ischemic stroke [14]. Budesonide-loaded SLN prepared by emulsification-solvent diffusion method was developed to deliver drugs to the lungs; hence SLN was explored for delivering drugs to various targets by solving the solubility problem of the drug as well as by using nanometric size advantages [15]. Antiviral drug Acyclovir was also loaded into SLN prepared by using fractionated coconut oil fabricated in two batches using Glyceryl Monostearate and lipid S75, focusing on the

preparation of SLN by high-pressure homogenization process [16, 17]. Lipid nanoparticles are a superior substitute for transdermal medication delivery [18, 19]. It is also possible to reduce P-glycoprotein-mediated drug efflux of multidrug-resistant malignant cells by using SLN-containing doxorubicin [20].

To produce smaller particles and a homogenous dispersion, the synthesis of solid lipid nanoparticles is being investigated. The solid lipid nanoparticle's stability is further enhanced by the process factors. The solid lipid nanoparticle can be created by using high-energy techniques like high-pressure homogenization and microfluidization. The phase inversion temperature method is one low-energy technique that modifies the solubility of polyethoxylated non-ionic surfactants by varying temperatures [21, 22]. Hydrophilic drug loading into a lipid matrix is difficult [23, 24]. To prepare gemcitabine-loaded solid lipid nanoparticles (SLNs), Nandini *et al.* used a double emulsification process with stearic acid as the lipid, soy lecithin as the surfactant, and sodium taurocholate as the cosurfactant. Over the course of three months, the stability study was conducted, and the results showed that there was very little change in the entrapment efficiency at 25±2 °C/60±5% RH, but no observable change in the particle size [25]. According to a report, lipid was used to prepare elvitegravir-loaded solid lipid nanoparticles, and its effects on drug release kinetics, zeta potential, polydispersity index, and particle size were assessed. Following this, the impact of a cryoprotectant was noted on these parameters [26].

Rosuvastatin is an antihyperlipidemic drug used to treat high cholesterol and triglyceride levels and is a BCS-II class drug with solubility issues due to its crystalline nature [27]. The research papers suggest Rosuvastatin can be utilized as an anticancer as well [28]. The bioavailability is also affected by factors like stomach acid susceptibility and first-pass metabolism [28]. Rosuvastatin, undergoes extensive first-pass metabolism after oral administration, with a 20% oral bioavailability. It is bound to plasma protein, mainly serum albumin, and excreted 90% in feces, with a 19 h elimination half-life [28]. Lipid-based delivery methods reduce hepatic first-pass

metabolism and increase oral bioavailability by transferring drugs through intestinal lymph vesicles, which drain directly into the thoracic duct and subsequently into the venous blood, avoiding the portal circulation [29, 30]. The objective of this study is to optimize the drug's release characteristics, which will increase its bioavailability and eventually improve its efficacy [31, 32].

MATERIALS AND METHODS

The supplier of rosuvastatin calcium was Yarrow Chemical Limited in Mumbai, India. The supplier of glyceryl monostearate was Otto Chemicals Limited in Mumbai, India. A complimentary sample of Kolliphor RH 40 was provided by Zeel Chemicals in Mumbai, India. The other compounds were analytically graded.

Optimization

The experimental proceedings were designed using the approach of central composite design (CCD). The dependent variables were mean dissolution time and entrapment efficiency. The independent variables were lipid and emulsifier concentration. Table 1 summarizes the account of 13 experiments. All the experiments were done in triplicate a crucial component of the response surface approach is the CCD model. Another name for the CCD model is the A Box-Wilson Central Composite Design. The response surface plot may be determined with the assistance of the center point, which represents the experimental domain, and the star point outside of it. The specific features needed for the design determine the exact value of α [31, 32]. The variables used in this experiment were lipid and emulsifier as independent variables and mean dissolution time

and entrapment efficiency as dependent variables. The lipid used in this study was glyceryl monostearate and the emulsifier was Kolliphor RH 40. The study used software (Design Expert v13) to generate response surface plots and numerically optimize new formulations with desired responses. The software sorted solutions descending by desirability, and significant factors were identified using ANOVA.

The process of preparation of solid lipid nanoparticles also impacts the entrapment efficiency [33] mean dissolution time and hence, the variables selected are entrapment efficiency and mean dissolution time in this study.

Solid lipid nanoparticle preparation

The weighed amount of the drug (10 mg) was taken in a beaker and the required amount of lipid was added to the formulation as per the formula given in table 1. This drug and lipid were mixed properly under heat at 90 °C until the drug got solubilized. The water was heated at 70 °C and an emulsifier was added to the mixture. The above mixture was mixed and stirred. The obtained dispersion was cooled until the solution was changed from turbid to transparent. The Phase inversion temperature was obtained by measuring the conductivity as the emulsion changes from w/o to o/w type emulsion [34-36]. The lipid was selected based on the solubility of the drug, stearic acid and glyceryl monostearate were chosen and the drug dissolved in glyceryl monostearate was more in quantity as compared to stearic acid. The emulsifier was chosen based on the clarity of the formulation prepared. The emulsifiers were Kolliphor RH 40 and Tween 80.

Table 1: The coded values and actual values of formulations generated by central composite design

S. No.	Lipid (Coded value)	Lipid (Actual value)	Emulsifier (Coded value)	Emulsifier (Actual value)
1	-1.41	23.12 mg	0	200 mg
2	1	100 mg	1	250 mg
3	1.41	203.12	0	200 mg
4	1	100 mg	-1	150 mg
5	0	90 mg	0	200 mg
6	0	90 mg	0	200 mg
7	0	90 mg	1.41	412.1 mg
8	-1	80 mg	1	250 mg
9	0	90 mg	0	200 mg
10	0	90 mg	0	200 mg
11	0	90 mg	-1.41	12.1 mg
12	0	90 mg	0	200 mg
13	-1	80 mg	-1	150 mg

The lowest coded value is coded as -1 and the highest value is 1, CCD uses α values, which can be negative (coded as -1.41) and positive (1.41) as well. The α value is outside the design space, calculated based on the lowest value and highest value concerning the middle value (0). The actual lowest and actual highest value was selected based on a trial run (table 1).

Characterization

Entrapment efficiency

All of the software-generated formulas that made up the dispersion were placed in a centrifuge tube and spun for 90 min at 15000 RPM. After removing the supernatant liquid, the amount of free drug was calculated. For every formulation, this was done [37]. Table 2 summarizes the data obtained.

$$EE = \frac{(\text{Total drug conc} - \text{Supernatant drug conc})}{\text{Total drug conc}} * 100$$

Dissolution

Using basket-type dissolution equipment, an *in vitro* release study of solid lipid nanoparticles (SLN-RC) loaded with rosuvastatin was conducted for 24 h. The dispersion was taken in a dialysis membrane and Phosphate buffer 6.8 as the dissolution media, the total drug in the formulation was 10 mg. The release study was done

using 500 ml of Phosphate buffer and aliquots of samples were collected at predetermined points. Phosphate buffer 6.8 was added to the media to maintain sink condition. The obtained data was analyzed for mean Dissolution time (MDT) in table 2 [38].

Characterization of optimized formulation

Particle size and zeta potential

Using a Malvern Zetasizer, the SLN-RC optimized formulation's mean particle size and Zeta Potential were determined. Double-distilled water was used to dilute each sample so that their concentration was appropriate for analysis [39].

X-ray diffraction (XRD)

Lipid nanoparticles have crystalline structure and the lattice structure is predominantly important for the drug to stay trapped in the lattice. Expulsion of the drug from the lattice may alter the release pattern of the formulation. The XRD is done as per the protocol [40].

Differential scanning calorimetry

Differential Scanning Calorimetry (DSC) is used as a tool to study interaction in the formulation. The optimized formulation was taken for analysis. The DSC graph obtained was interpreted for more details of lipid melting behaviour [41].

Fourier transform infrared spectroscopy (FTIR)

The optimized formulation was analyzed to confirm their intermolecular interactions. The dried samples were prepared using Potassium bromide to form pellets.

Transmission electron microscopy

To improve the targeting and localization of therapeutic molecules, it is crucial to analyze the internal lipid matrix organization of solid-state nanomedicines (SLNs) using TEM, an effective technique for doing so [6]. To conduct a TEM study, a 0.4% (w/v) SLN dispersion with the necessary dilution was scattered on a 300 mesh size, 3 mmol formvar-coated copper grid and stained with 4% uranyl acetate for 30 seconds before being dried and subjected to analysis at an accelerating voltage of 100 kV.

RESULTS

Optimization

Formulation variables like lipid concentration and emulsifier concentration were considered independent variables in this design (Central Composite Design). Various parameters were optimized keeping other constants. The various formulation and process variables were employed to obtain nanosized particles with maximum entrapment efficiency and mean dissolution time. The model summary for each responses are tabulated in tables 3 and 4. Lipid concentration was set to maximum for maximum entrapment of the drug. The Emulsifier was set to a minimum for the least toxicity [42, 43]. However, the concentration of lipids was seen to be significantly affecting the entrapment efficiency [44, 45]. Emulsifiers are known to reduce particle size which in turn can affect drug entrapment.

The independent variables were set according to the design space and dependent variables were also set. The software generated the formulation combinations. The 13-formulation combination had points outside the design space (1.41 and -1.41). The highest coded value inside the design space was 1 and the lowest coded value inside the design space was -1.

The obtained values for entrapment efficiency were tabulated and the linear model had a value of 0.9975, adjusted R^2 was 0.9970, and predicted R^2 was 0.9962 tabulated in Table 3. The equation for entrapment efficiency is $+80.76231 + 6.64413 * \text{lipid} - 0.17965 * \text{emulsifier}$. The data generated are listed in table no-3. Prob>F is the p-value for the whole model test. The value of "prob>F" is 0.0001. Value of "prob>F" less than 0.0500 indicate model terms are significant value greater than 0.1000 indicate the model terms are not significant. The "prob>F" value for lack of fit is 0.8614, which indicates lack of fit is not significant, which is good for the model. The comparative study of entrapment efficiency is done in fig. 1.

The obtained values for mean dissolution time were tabulated and the linear model had an R^2 value of 0.94, adjusted R^2 was 0.89, and predicted R^2 was 0.62. The equation for MDT = $+7.56000 + 0.509 * \text{lipid} - 8.21068E003 * \text{emulsifier} + 0.025000 * \text{lipid} * \text{emulsifier} + 0.30125 * \text{lipid}^2 - 0.098750 * \text{emulsifier}^2$. The p-value of the mean dissolution time was 0.0004. Suggesting that the data was best fitting in the quadratic model. The p-value for lack of fit was 0.0517. The lack of fit insignificant supports the proceedings of the experiment. The data generated are listed in table 4.

The mean dissolution time was found to be in the range of 7.1 ± 0.5 to 8.9 ± 0.6 . The lowest value was found to be in low coded value (-1, -1). The highest value was found to be in (1.41, 0). The optimization was carried out maximizing the lipid concentration and minimizing the emulsifier concentration. The value of "prob>F" is 0.0004. Value of "prob>F" less than 0.0500. The "prob>F" value for lack of fit is 0.0517. The optimized formulation selected was +1, -1 (lipid, emulsifier). The 3D graph (fig. 2) suggests the effect of lipid and emulsifier effect on responses like entrapment efficiency percentage and mean dissolution time.

The dissolution data was plotted, and the regression of each kinetic model was found. The drug release pattern of the formulations is depicted as an 8-hour sustained release observed in fig. 3 and the release kinetics of the formulation was studied in fig. 4.

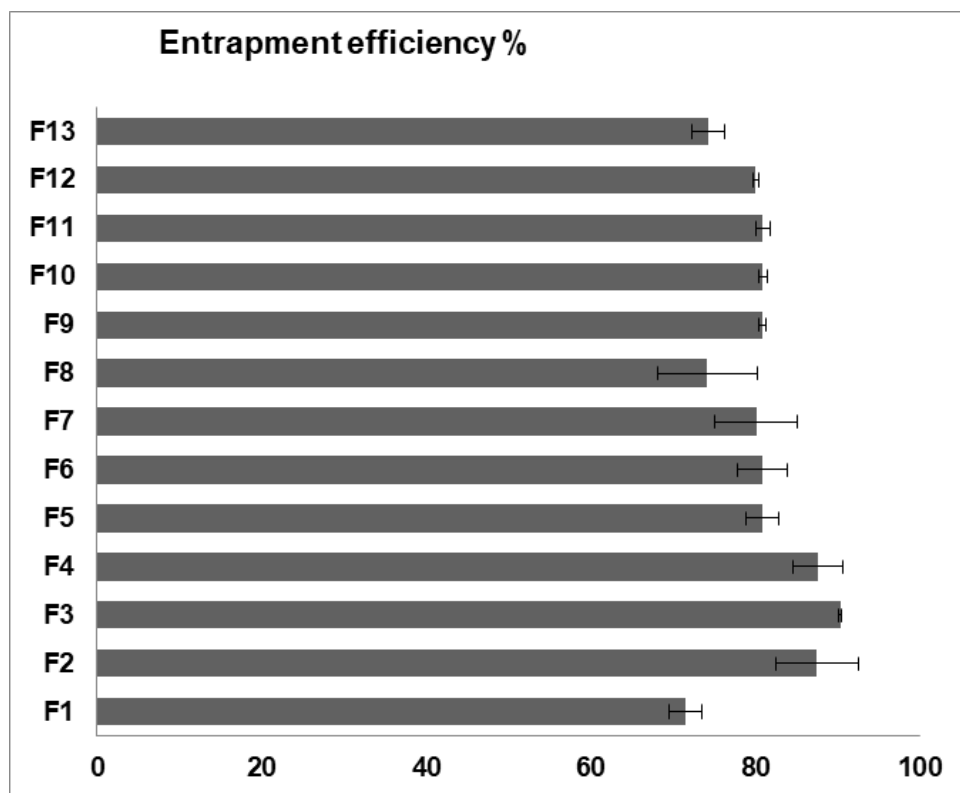


Fig. 1: Graph for entrapment efficiency % with SEM. The entrapment efficiency evaluation was performed in triplicate and average data was used for optimizing

Table 2: Responses of all formulations according to design space

S. No.	Lipid (Coded value)	Emulsifier (Coded value)	Entrapment efficiency %	Mean dissolution time (h)
1	-1.41	0	71.49+2	7.5+0.1
2	1	1	87.45+5	8.4+0.4
3	1.41	0	90.28+0.2	8.9+0.2
4	1	-1	87.61+3	8.1+0.1
5	0	0	80.89+2	7.6+0.6
6	0	0	80.89+3	7.6+0.2
7	0	1.41	80.1+5	7.2+0.4
8	-1	1	74.16+6	7.3+0.6
9	0	0	80.89+0.4	7.6+0.4
10	0	0	80.89+0.5	7.6+0.5
11	0	-1.41	80.89+0.9	7.6+0.5
12	0	0	80.05+0.4	7.4+0.2
13	-1	-1	74.32+2	7.1+0.1

The prepared formulation was analyzed and the observed data was tabulated along with the Standard deviation. All the experiments were performed in triplicate. The data is enumerated with±SD.

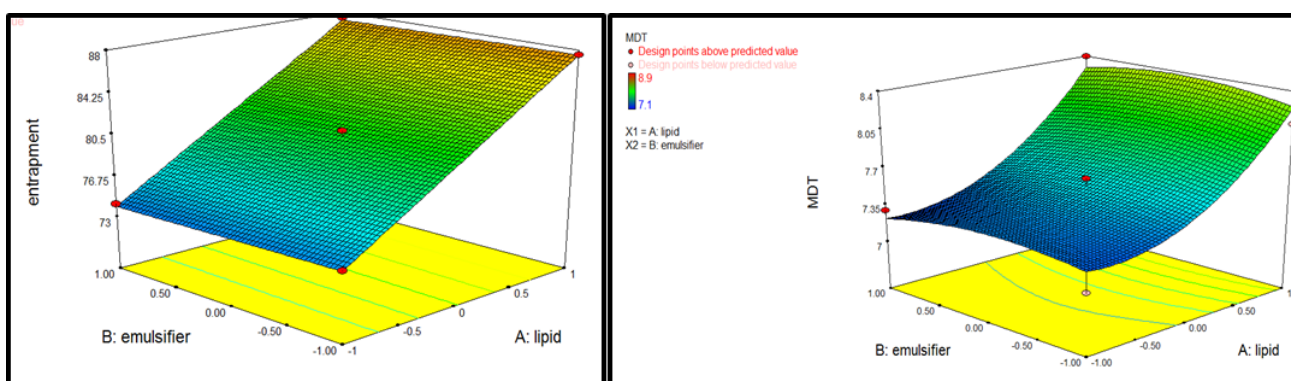


Fig. 2: 3D graph for entrapment efficiency, Mean dissolution time (MDT). The linear model for entrapment efficiency is evident from the 3D graph. The quadratic nature of the mean dissolution time explains that an increase in lipid increases the mean dissolution time, albeit in a quadratic nature. The emulsifier concentration has a less significant contribution as compared to the lipid concentration

Table 3: Model summary for entrapment efficiency %

Source	Std.	R-squared	Adjusted R-squared	Predicted R-squared
Linear	0.2975	0.9975	0.9970	0.9962
2FI	0.3136	0.9975	0.9967	0.9952
Quadratic	0.3207	0.9980	0.9965	0.9944
Cubic	0.3579	0.9982	0.9957	0.9838

Table 4: Model summary for mean dissolution time

Source	Std Dev.	R-squared	Adjusted R-squared	Predicted R-squared
Linear	0.31	0.69	0.62	0.34
2FI	0.33	0.69	0.58	0.26
Quadratic	0.16	0.94	0.89	0.62
Cubic	0.09	0.99	0.97	0.75

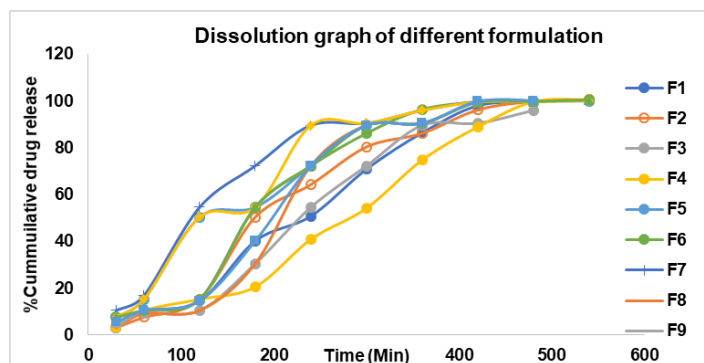


Fig. 3: Cumulative drug release graph. The dissolution was performed in triplicate and the average data for each formulation was used for plotting the cumulative release graph

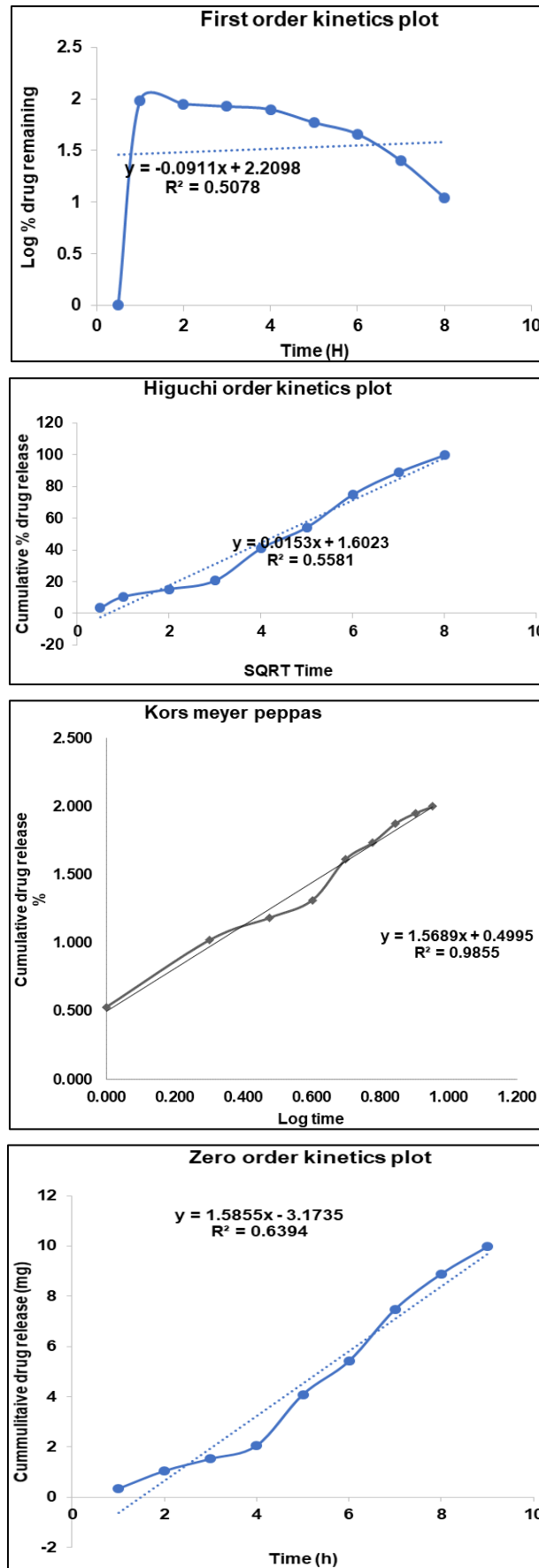


Fig. 4: Kinetic model graph of the optimized formulation; the optimized formulation was used for determining the kinetic model, the dissolution was performed in triplicate. The R² value for all the formulations was calculated. The R² value for the Korsmeier Peppas model was found to be highest is 0.9855

Particle size and zeta potential

Particle Size distribution of the optimized formulation was performed using the dynamic light scattering method. The particle size of the optimized formulation was 16.16 ± 10 nm and the particle size distribution index to 0.729 ± 0.02 . The Zeta Potential value was found to be -25.43 V. Fig. 5 shows the particle size of the optimized formulation and the zeta potential.

X-ray diffraction (XRD)

The diffraction peaks at 2θ values of 4.5, 16.04, 22.45, and 34.3, whereas nanoparticles showed a sharp peak at 22.78.

Differential scanning calorimetry

The stability of the complex formed between the drug and lipid was analyzed by Thermal analysis, and rosuvastatin calcium-loaded nanoparticles were subjected to DSC thermograms.

FTIR

3376 , 2932 , 1437 , 1336 , and 1230 cm^{-1} for rosuvastatin as per literature, characteristic peaks are present in the optimized formulation, indicating the absence of interaction.[52] fig. 6 depicts the XRD, DSC, and FTIR of the optimized formulation.

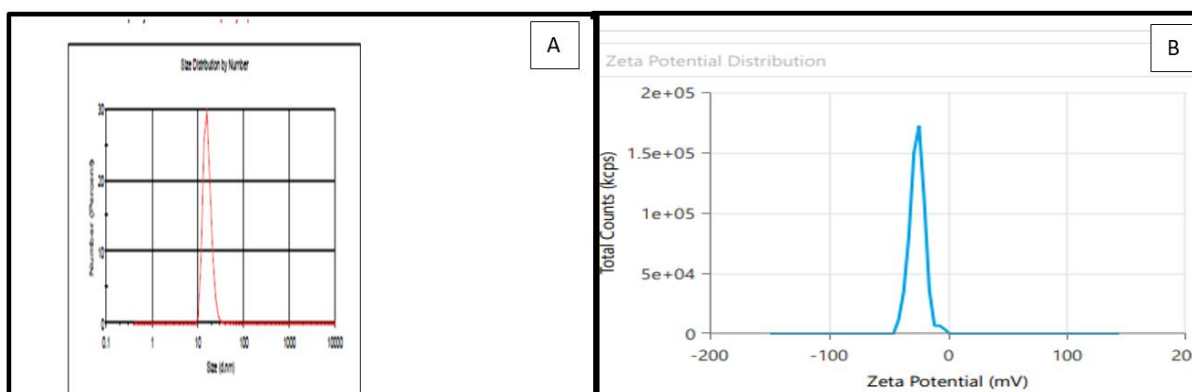


Fig. 5: a. Particle size of optimized formulation. b. Zeta potential of the optimized formulation the optimized formulation was diluted 10² times with Millipore water for both the characterization

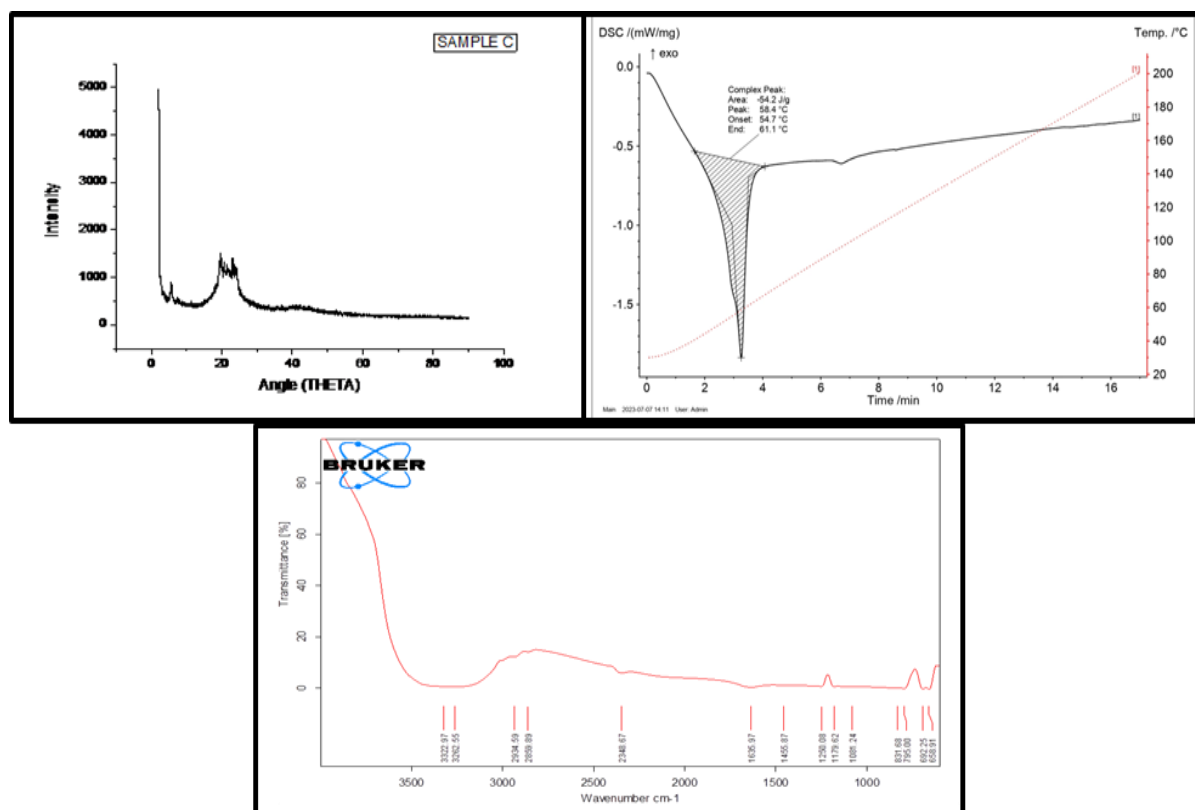


Fig. 6: XRD, DSC, FTIR plot of optimized formulation lyophilized

Transmission electron microscopy

Transmission electron microscopy of the optimized formulation was done to enable us to recognize morphological changes and particle

size of the nanoparticles. From the TEM micrograph investigation fig. 7, we observed that the particles get aggregated to each other even after sonication, which may be due to the small particle sizes of the nanoparticles.

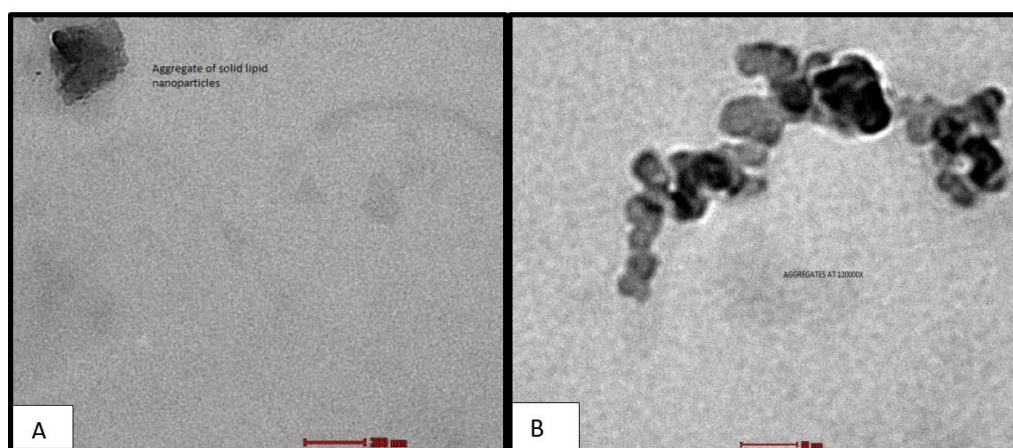


Fig. 7: A. Solid lipid nanoparticles Image under 45000X, B. Solid lipid nanoparticles under 120000X. The freshly prepared formulation dispersion was sent to the testing laboratory. The particle observed in the fig. was within in range of 50 nm. The small particle size of the nanoparticle was responsible for aggregation may be due to electrostatic forces. Increasing the zeta potential may prevent aggregation

DISCUSSION

Rosuvastatin is a statin drug with poor solubility, extensive first-pass metabolism, and poor oral bioavailability of 20%. The solid nanoparticle of rosuvastatin was prepared by employing glyceryl monostearate and Kolliphor RH 40. The solid lipid nanoparticle was prepared and the formulation using entrapment efficiency percentage and mean dissolution time as independent variable, by employing Design Expert v13 optimizing software. The data for entrapment efficiency percentage was best fitting in a linear model. This is in support of the effect of lipid concentration variation that an increase in lipid concentration provides more lipid matrix for the lipophilic drug to stay embedded; as the concentration was increased or high coded value (1.41 in central composite design) had the highest value $90.28\% \pm 0.84$. The lowest value was found to be $71.49\% \pm 0.62$. The mean value for entrapment efficiency was found to be 80.76%, with a standard deviation of 5.43. The linear model had p value < 0.0001 suggesting significant data. The lowest value was obtained from the formulation with the lowest coded value (-1.41 in central composite design) and emulsifier of medium range (0). The points in the central composite design, like alpha or 1.41/-1.41 create noise or multicollinearity, disrupting the model coefficient estimation equation. The Regression analysis of responses and standard deviation was tabulated in table 3 and 4. R^2 indicates the correlation between the predicted value and the actual value. The equation depicts the effect of different variables, the model is selected based on the regression value obtained by analyzing the responses, and the selected model has a regression value nearer to 1. The adjusted R^2 should be closer to the predicted R^2 which indicates the robustness of the evaluation process. Hence, a linear model was selected for entrapment efficiency and a quadratic model for mean dissolution time. The value of "Prob>F" is 0.0001. Value of "Prob>F" less than 0.0500 indicate model terms are significant. Value greater than 0.1000 indicate the model terms are not significant. The "Prob>F" value for lack of fit is 0.8614 which indicates lack of fit is not significant which is good for the model. A significant lack of fit test indicates that the variation of design points around their predicted values is larger than that of replicates around their mean values. The optimization was carried out maximizing the lipid concentration and minimizing the emulsifier concentration. The value of "Prob>F" is 0.0004. The lowest and highest values obtained from the experiment are indicative of the effect of the concentration of lipids predominantly involved in entrapping the drug in the lipid matrix [46]. This is also observed from the 3D graph (fig. 1) obtained from the optimization software. The 3D graph depicts the effect of lipid and emulsifier concentration on entrapment efficiency. The increase in lipid concentration results in the entrapment of the drug in a lipid matrix, whereas the emulsifier does not have such a prominent influence on the entrapment efficiency of the solid lipid nanoparticles formed [47-49].

Entrapment efficiency percentage is influenced by various factors such as lipid material types, composition, crystallinity, and drug solubility in both organic and aqueous phases. The molten lipid accommodates the drug in the lipid matrix and the position of the drug in the nanoparticle determines the pattern of *in vitro* and *in vivo* drug release. The positive value associated with lipid concentration in the equation is in support of the obtained results. The emulsifier concentration is significant as it decreases the surface tension and increases the surface area [50].

The mean dissolution time was found to be in the range of 7.1 ± 0.5 to 8.9 ± 0.6 . The lowest value was found to be in low coded value (-1,-1). The highest value was found to be in (1.41,0). This demonstrates the effect of solid lipids in entrapping the drug and subsequent release of the drug. This is also observed from a 3D graph (fig. 2) obtained from the optimization software. The mean dissolution time of a drug is determined by its dose/solubility ratio, which estimates the volume of fluids needed to dissolve an individual dose. MDT measures drug release rate and polymer retarding efficacy, with higher MDT indicating better drug-retarding ability and vice versa. The release kinetics of the optimized formulation is found to be following the korsmeyer peppas model as the R^2 is found to be 0.9855. This indicates that swelling of the solid lipid nanoparticle before the drug is released into the dissolution media.

The long-term stability of the colloidal system can be inferred from the measurements of the zeta potential [51]. There is unlikely to be a tendency for the particles in suspension to repel one another if they all have a high negative or positive value. However, there isn't any force to stop the particles from aggregating and flocculating if their zeta potential values are substantially low [52]. Thus, the zeta potential and size are crucial for the efficacy of nanoparticles in drug delivery. The particle size of the optimized formulation was 16.16 ± 10 and the particle size distribution index to 0.729 ± 0.02 . The Zeta Potential value was found to be -25.43 mV. It is reported that higher zeta potential is essential to keep the particles from aggregating. Higher Zeta Potential and particle size greater than 50 nm are reported to be better in terms of bioavailability [53]. Apostolour *et al.* found that SLN particle size is influenced by the structure and melting point of solid lipids, with smaller sizes resulting from simpler molecules [54]. Dhoranwala *et al.* optimized solid lipid nanoparticles of Rosuvastatin using full factorial design using glyceryl monostearate and Poloxamer 188 with enhanced stability [55]. Studies have reported the effect of lipids on particle size; the increase in lipid concentration increased the particle size, whereas the size reduced with increasing the surfactant concentration [56-58]. Danei *et al.* 2018 reported that particle size and particle size distribution index can be utilized to deliver lipidic nanocarriers to different sites like kidney, liver, pulmonary, and tumor sites [59].

Nanoparticulate rosuvastatin is reported to have a better dissolution profile than untreated rosuvastatin calcium [60]. The presence of XRD peak of 22.78° indicates the nanoparticles. The solid lipid glyceryl monostearate shows an XRD peak of 40.89Å, DSC of the optimized formulation has shown a peak at 58 °C, indicating the presence of the drug enclosed in the solid lipid [61]. Keshwarwani *et al.* reported that the prepared solid lipid nanoparticle had a different peak than that of the drug, indicating that the drug was dissolved in lipid [62]. 3376, 2932, 1437, 1336, and 1230 cm⁻¹ for rosuvastatin as per literature, characteristic peaks are present in the optimized formulation, indicating the absence of interaction [63]. The presence of a peak around 3400 indicates the presence of water molecules supported by the work done by Talele *et al.*, 2018 [10]. The solid lipid nanoparticle had the drug enclosed in the lipid matrix rather than distributed uniformly in the lipid matrix. This can be also supported by the pattern of release of drugs in the cumulative drug release graph. There is a slow release initially, then a slight increase around 400 min and complete release occurs between 500 min to 600 min. The hydrophobic core region of SLN and the hydrophilic peripheral region with the glycerol backbone indicate the presence of bound-water molecules [10].

The image under 120000X shows aggregated particles under the size of 50 nm, this may be due to the electrostatic attraction between the nanoparticles as the size is small. The lipid crystals were not visible in the image, indicating that crystallization of lipids did not occur [64-66]. Another study demonstrated the enhanced bioavailability of solid lipid nanoparticles (RC-SLNs) compared to the drug suspension after oral administration of Wistar rats [67].

The process employed in this study involves heat but is as not high as the hot homogenization process. The drug stability is not compromised as expected in the hot homogenization process. The drug expulsion from the lattice of lipids is a major limitation associated with solid lipid nanoparticles [4]. The particle size obtained in this study is smaller in size hence, this could be utilized for sustained release of the drug over a longer period. SLNs have limitations such as limited component binding, component damage, low loading capacity, and water requirement for dissolution. They can also experience lipid particle growth, unpredictable lipid transition dynamics, and low binding ability [68-70].

CONCLUSION

The solid lipid nanoparticle of Rosuvastatin is prepared successfully. The concentration of solid lipid and emulsifier was optimized, setting the emulsifier as low due to the toxicity attributes of emulsifiers. The method of preparation of solid lipid nanoparticles is also vital and the method used here is phase inversion temperature, which is convenient and produces reduced particle size of nanoparticles. The Transmission electron microscopy images show smaller particle sizes. The release pattern of the drug from the formulation is important since the drug needs to be released in a sustained manner to avoid toxicity. The physicochemical properties of a drug must be unaltered to get the desired therapeutic effect, the formulation maintains the physicochemical property of the drug and hence, this formulation can further be evaluated for long-term stability. The study concludes that the solubility and dissolution rate of rosuvastatin can be enhanced by preparing Solid lipid nanoparticles while using glyceryl monostearate as a solid lipid and Kolliphor RH40 as the emulsifier. The study can be fabricated by alteration of solid lipids and emulsifiers. The process control attributes must be involved in the future study with its effect on major responses like particle size and zeta potential. The solid lipid nanoparticle *in vivo* study of the newer researched potential of Rosuvastatin calcium may be explored.

ACKNOWLEDGEMENT

We are thankful to Central Instrumentation Laboratory (CIL) Central University of Punjab for XRD; Sophisticated Test and Instrumentation Centre, CUSAT for DSC and FTIR; SN Bose Institute Kolkata for Particle Size analysis; Indian Association For The Cultivation Of Science, Kolkata for Zeta Potential; Jamia Hamdard University, Delhi for TEM analysis.

ABBREVIATION

SLN-Solid Lipid Nanoparticle, BCS-Biopharmaceutical Classification System, MDT-mean Dissolution Time, DSC-Differential Scanning

Calorimetry, FTIR-Fourier Transform Infrared Spectroscopy, DTX-Docetaxel, CCD-Central Composite Design, EE-Entrapment Efficiency, SLN-RC-Solid Lipid Nanoparticle Rosuvastatin loaded, TEM-Transmission Electron Microscopy, 3D-3 Dimension, CIL-Central Instrumentation Laboratory, XRD-X-Ray Diffraction, RH-Relative Humidity, ANOVA-Analysis of Variance, RPM-Rotation per Minute, SD-Standard Deviation, SEM-Standard Error Mean, CVD-cardiovascular diseases

FUNDING

Nil

AUTHORS CONTRIBUTIONS

P C reviewed the paper. CMH evaluated the protocol and data, along with reviewing the writing of the paper and communication to the journal. DD experimented and drafted the paper.

CONFLICT OF INTERESTS

Declared none

REFERENCES

1. DE Jong WH, Borm PJ. Drug delivery and nanoparticles: applications and hazards. *Int J Nanomedicine*. 2008;3(2):133-49. doi: [10.2147/ijn.s596](https://doi.org/10.2147/ijn.s596), PMID [18686775](https://pubmed.ncbi.nlm.nih.gov/18686775/), PMCID [PMC2527668](https://pubmed.ncbi.nlm.nih.gov/PMC2527668/).
2. Ghasemiyeh P, Mohammadi Samani S. Solid lipid nanoparticles and nanostructured lipid carriers as novel drug delivery systems: applications advantages and disadvantages. *Res Pharm Sci*. 2018 Aug;13(4):288-303. doi: [10.4103/1735-5362.235156](https://doi.org/10.4103/1735-5362.235156), PMID [30065762](https://pubmed.ncbi.nlm.nih.gov/30065762/).
3. Elmowafy M, Al Sanea MM. Nanostructured lipid carriers (NLCs) as drug delivery platform: advances in formulation and delivery strategies. *Saudi Pharm J*. 2021 Sep;29(9):999-1012. doi: [10.1016/j.jsps.2021.07.015](https://doi.org/10.1016/j.jsps.2021.07.015), PMID [34588846](https://pubmed.ncbi.nlm.nih.gov/34588846/).
4. Mukherjee S, Ray S, Thakur RS. Solid lipid nanoparticles: a modern formulation approach in drug delivery system. *Indian J Pharm Sci*. 2009 Jul;71(4):349-58. doi: [10.4103/0250-474X.57282](https://doi.org/10.4103/0250-474X.57282), PMID [20502539](https://pubmed.ncbi.nlm.nih.gov/20502539/).
5. Naseri N, Valizadeh H, Zakeri Milani P. Solid lipid nanoparticles and nanostructured lipid carriers: structure preparation and application. *Adv Pharm Bull*. 2015 Sep;5(3):305-13. doi: [10.15171/apb.2015.043](https://doi.org/10.15171/apb.2015.043), PMID [26504751](https://pubmed.ncbi.nlm.nih.gov/26504751/).
6. Dawoud MH, Fayed AM, Mohamed RA, Sweed NM. Enhancement of the solubility of rosuvastatin calcium by nanovesicular formulation: a systematic study based on a quality by design approach. *Proceedings*. 2021;78(1):34. doi: [10.3390/IECP2020-08698](https://doi.org/10.3390/IECP2020-08698).
7. MA P, Dong X, Swadley CL, Gupte A, Leggas M, Ledebur HC. Development of idarubicin and doxorubicin solid lipid nanoparticles to overcome Pgp mediated multiple drug resistance in leukemia. *J Biomed Nanotechnol*. 2009 Apr;5(2):151-61. doi: [10.1166/jbn.2009.1021](https://doi.org/10.1166/jbn.2009.1021), PMID [20055093](https://pubmed.ncbi.nlm.nih.gov/20055093/).
8. El Telbany DF, El Telbany RF, Zakaria S, Ahmed KA, El Feky YA. Formulation and assessment of hydroxyzine HCl solid lipid nanoparticles by dual emulsification technique for transdermal delivery. *Biomed Pharmacother*. 2021 Nov;143:112130. doi: [10.1016/j.biopha.2021.112130](https://doi.org/10.1016/j.biopha.2021.112130), PMID [34560549](https://pubmed.ncbi.nlm.nih.gov/34560549/).
9. Rai N, Madni A, Faisal A, Jamshaid T, Khan MI, Khan MM. Glyceryl monostearate-based solid lipid nanoparticles for controlled delivery of docetaxel. *Curr Drug Deliv*. 2021;18(9):1368-76. doi: [10.2174/1567201818666210203180153](https://doi.org/10.2174/1567201818666210203180153), PMID [33538673](https://pubmed.ncbi.nlm.nih.gov/33538673/).
10. Talele P, Sahu S, Mishra AK. Physicochemical characterization of solid lipid nanoparticles comprised of glycerol monostearate and bile salts. *Colloids Surf B Biointerfaces*. 2018 Dec 1;172:517-25. doi: [10.1016/j.colsurfb.2018.08.067](https://doi.org/10.1016/j.colsurfb.2018.08.067), PMID [30212689](https://pubmed.ncbi.nlm.nih.gov/30212689/).
11. HE J, Huang S, Sun X, Han L, Chang C, Zhang W. Carvacrol loaded solid lipid nanoparticles of propylene glycol monopalmitate and glyceryl monostearate: preparation characterization and synergistic antimicrobial activity. *Nanomaterials (Basel)*. 2019;9(8):1162. doi: [10.3390/nano9081162](https://doi.org/10.3390/nano9081162), PMID [31416170](https://pubmed.ncbi.nlm.nih.gov/31416170/).
12. Torrado Salmeron C, Guarnizo Herrero V, Torrado G, Pena MA, Torrado-Santiago S, DE LA Torre Iglesias PM. Solid dispersions of atorvastatin with kolliphor RH40: enhanced supersaturation and improvement in a hyperlipidemic rat model. *Int J Pharm*. 2023 Jan 25;631:122520. doi: [10.1016/j.ijpharm.2022.122520](https://doi.org/10.1016/j.ijpharm.2022.122520), PMID [36581105](https://pubmed.ncbi.nlm.nih.gov/36581105/).

13. Yasir M, Chauhan I, Ameerduzzafar Z, Verma M, Noorulla KM, Abdurazak T, Nabil A, Misbahu H, Dinesh P, Gurmessa G, Debessa D, Sara UVS, Kumar N. Buspirone loaded solid lipid nanoparticles for amplification of nose to brain efficacy: formulation development optimization by box behnken design *in vitro* characterization and *in vivo* biological evaluation. *J Drug Deliv Sci Technol*. 2021 Feb;61:112164. doi: [10.1016/j.jddst.2020.102164](https://doi.org/10.1016/j.jddst.2020.102164).
14. Sohail S, Shah FA, Zaman SU, Almari AH, Malik I, Khan SA. Melatonin delivered in solid lipid nanoparticles ameliorated its neuroprotective effects in cerebral ischemia. *Heliyon*. 2023;9(9):e19779. doi: [10.1016/j.heliyon.2023.e19779](https://doi.org/10.1016/j.heliyon.2023.e19779), PMID [37809765](https://pubmed.ncbi.nlm.nih.gov/37809765/).
15. Emami J, Mohiti H, Hamishehkar H, Varshosaz J. Formulation and optimization of solid lipid nanoparticle formulation for pulmonary delivery of budesonide using taguchi and box behnken design. *Res Pharm Sci*. 2015;10(1):17-33. PMID [26430454](https://pubmed.ncbi.nlm.nih.gov/26430454/), PMCID [PMC4578209](https://pubmed.ncbi.nlm.nih.gov/PMC4578209/).
16. Dhiman N, Awasthi R, Sharma B, Kharkwal H, Kulkarni GT. Lipid nanoparticles as carriers for bioactive delivery. *Front Chem*. 2021 Apr 23;9:580118. doi: [10.3389/fchem.2021.580118](https://doi.org/10.3389/fchem.2021.580118), PMID [33981670](https://pubmed.ncbi.nlm.nih.gov/33981670/).
17. Bhupinder K, Newton MJ. Acyclovir solid lipid nanoparticles for skin drug delivery: fabrication characterization and *in vitro* study. *Recent Pat Drug Deliv Formul Pat. Drug*. 2017;11(2):132-46. doi: [10.2174/1872211311666170117123403](https://doi.org/10.2174/1872211311666170117123403), PMID [28124592](https://pubmed.ncbi.nlm.nih.gov/28124592/).
18. Stefanov SR, Andonova VY. Lipid nanoparticulate drug delivery systems: recent advances in the treatment of skin disorders. *Pharmaceuticals (Basel)*. 2021;14(11):1083. doi: [10.3390/ph14111083](https://doi.org/10.3390/ph14111083), PMID [34832865](https://pubmed.ncbi.nlm.nih.gov/34832865/), PMCID [PMC8619682](https://pubmed.ncbi.nlm.nih.gov/PMC8619682/).
19. Garg A, Sharma GS, Goyal AK, Ghosh G, SI SC, Rath G. Recent advances in topical carriers of anti-fungal agents. *Heliyon*. 2020;6(8):e04663. doi: [10.1016/j.heliyon.2020.e04663](https://doi.org/10.1016/j.heliyon.2020.e04663), PMID [32904164](https://pubmed.ncbi.nlm.nih.gov/32904164/).
20. Chen HH, Huang WC, Chiang WH, Liu TI, Shen MY, Hsu YH. pH responsive therapeutic solid lipid nanoparticles for reducing P-glycoprotein mediated drug efflux of multidrug-resistant cancer cells. *Int J Nanomedicine*. 2015;10:5035-48. doi: [10.2147/IJN.S86053](https://doi.org/10.2147/IJN.S86053), PMID [26346762](https://pubmed.ncbi.nlm.nih.gov/26346762/).
21. Kumar M, Bishnoi RS, Shukla AK, Jain CP. Techniques for formulation of nanoemulsion drug delivery system: a review. *Prev Nutr Food Sci*. 2019;24(3):225-34. doi: [10.3746/pnf.2019.24.3.225](https://doi.org/10.3746/pnf.2019.24.3.225), PMID [31608247](https://pubmed.ncbi.nlm.nih.gov/31608247/), PMCID [PMC6779084](https://pubmed.ncbi.nlm.nih.gov/PMC6779084/).
22. Song KC, HS Lee, IY Choung, KI Cho, Y Ahn, EJ Choi. The effect of type of organic phase solvents on the particle size of poly (d,l-lactide-co-glycolide) nanoparticles. *Colloids and Surfaces a: Physicochemical and Engineering Aspects*. 2006 Mar 15; 276(1-3):162-7. doi: [10.1016/j.colsurfa.2005.10.064](https://doi.org/10.1016/j.colsurfa.2005.10.064).
23. Weerapol Y, Manmuan S, Chaothanaphat N, Limmatvapirat S, Sirirak J, Tamdee P. New approach for preparing solid lipid nanoparticles with volatile oil loaded quercetin using the phase inversion temperature method. *Pharmaceutics*. 2022;14(10):1984. doi: [10.3390/pharmaceutics14101984](https://doi.org/10.3390/pharmaceutics14101984), PMID [36297420](https://pubmed.ncbi.nlm.nih.gov/36297420/), PMCID [PMC9607647](https://pubmed.ncbi.nlm.nih.gov/PMC9607647/).
24. Dara T, Vatanara A, Nabi Meybodi M, Vakilinezhad MA, Malvajerd SS, Vakhshiteh F. Erythropoietin loaded solid lipid nanoparticles: preparation optimization and *in vivo* evaluation. *Colloids Surf B Biointerfaces*. 2019 Jun 1;178:307-16. doi: [10.1016/j.colsurfb.2019.01.027](https://doi.org/10.1016/j.colsurfb.2019.01.027), PMID [30878805](https://pubmed.ncbi.nlm.nih.gov/30878805/).
25. Nandini PT, Doijad RC, Shivakumar HN, Dandagi PM. Formulation and evaluation of gemcitabine loaded solid lipid nanoparticles. *Drug Deliv*. 2015;22(5):647-51. doi: [10.3109/10717544.2013.860502](https://doi.org/10.3109/10717544.2013.860502), PMID [24283392](https://pubmed.ncbi.nlm.nih.gov/24283392/).
26. Kommavarapu P, Maruthapillai A, Palanisamy K. Preparation characterization and evaluation of elvitegravir loaded solid lipid nanoparticles for enhanced solubility and dissolution rate. *Trop J Pharm Res*. 2015;14(9):1549-56. doi: [10.4314/tjpr.v14i9.2](https://doi.org/10.4314/tjpr.v14i9.2).
27. Vemuri VD, Lankalapalli S. Cocrystal construction between rosuvastatin calcium and L-asparagine with enhanced solubility and dissolution rate. *Turk J Pharm Sci*. 2021;18(6):790-8. doi: [10.4274/tjps.galenos.2021.62333](https://doi.org/10.4274/tjps.galenos.2021.62333), PMID [34979738](https://pubmed.ncbi.nlm.nih.gov/34979738/).
28. Fatehi Hassanabad A. Current perspectives on statins as potential anticancer therapeutics: clinical outcomes and underlying molecular mechanisms. *Transl Lung Cancer Res*. 2019;8(5):692-9. doi: [10.21037/tlcr.2019.09.08](https://doi.org/10.21037/tlcr.2019.09.08), PMID [31737505](https://pubmed.ncbi.nlm.nih.gov/31737505/).
29. Ahmed TA, Elimam H, Alrifai AO, Nadhrh HM, Masoudi LY, Sairafi WO. Rosuvastatin lyophilized tablets loaded with flexible chitosomes for improved drug bioavailability anti-hyperlipidemic and anti-oxidant activity. *Int J Pharm*. 2020 Oct 15;588:119791. doi: [10.1016/j.ijpharm.2020.119791](https://doi.org/10.1016/j.ijpharm.2020.119791), PMID [32827673](https://pubmed.ncbi.nlm.nih.gov/32827673/).
30. Ahmed TA. Development of rosuvastatin flexible lipid-based nanoparticles: promising nanocarriers for improving intestinal cells cytotoxicity. *BMC Pharmacol Toxicol*. 2020;21(1):14. doi: [10.1186/s40360-020-0393-8](https://doi.org/10.1186/s40360-020-0393-8), PMID [32085802](https://pubmed.ncbi.nlm.nih.gov/32085802/).
31. Yanez JA, Wang SW, Knemeyer IW, Wirth MA, Alton KB. Intestinal lymphatic transport for drug delivery. *Adv Drug Deliv Rev*. 2011;63(10-11):923-42. doi: [10.1016/j.addr.2011.05.019](https://doi.org/10.1016/j.addr.2011.05.019), PMID [21689702](https://pubmed.ncbi.nlm.nih.gov/21689702/).
32. Zhang Z, LU Y, QI J, WU W. An update on oral drug delivery via intestinal lymphatic transport. *Acta Pharm Sin B*. 2021;11(8):2449-68. doi: [10.1016/j.apsb.2020.12.022](https://doi.org/10.1016/j.apsb.2020.12.022), PMID [34522594](https://pubmed.ncbi.nlm.nih.gov/34522594/).
33. Nguyen TT, Duong VA. Solid lipid nanoparticles. *Encyclopedia*. 2022;2(2):952-73. doi: [10.3390/encyclopedia2020063](https://doi.org/10.3390/encyclopedia2020063).
34. Gulati P, Dewangan HK. Aceclofenac loaded solid lipid nanoparticles: optimization *in vitro* and *ex-vivo* evaluation. *Int J App Pharm*. 2023;15(4):184-90. doi: [10.22159/ijap.2023v15i4.48047](https://doi.org/10.22159/ijap.2023v15i4.48047).
35. Granato D, Calado V. The use and importance of design of experiments (DOE) in process modeling in food science and technology. In: *Mathematical and Statistical Methods in Food Science and Technology*. 2014;1:1-18. doi: [10.1002/9781118434635.ch1](https://doi.org/10.1002/9781118434635.ch1).
36. Bevilacqua A, Corbo MR, Sinigaglia M. Design of experiments: a powerful tool in food microbiology; 2010. p. 1419-29.
37. Onugwu AL, Attama AA, Nnamani PO, Onugwu SO, Onuigbo EB, Khutoryanskiy VV. Development and optimization of solid lipid nanoparticles coated with chitosan and poly (2-ethyl-2-oxazoline) for ocular drug delivery of ciprofloxacin. *Journal of Drug Delivery Science and Technology*. 2022 Aug;74:103527. doi: [10.1016/j.jddst.2022.103527](https://doi.org/10.1016/j.jddst.2022.103527).
38. Ortiz AC, Yanez O, Salas Huenuleo E, Morales JO. Development of a nanostructured lipid carrier (NLC) by a low energy method comparison of release kinetics and molecular dynamics simulation. *Pharmaceutics*. 2021;13(4):531. doi: [10.3390/pharmaceutics13040531](https://doi.org/10.3390/pharmaceutics13040531), PMID [33920242](https://pubmed.ncbi.nlm.nih.gov/33920242/).
39. Rohit B, Pal KI. A method to prepare solid lipid nanoparticles with improved entrapment efficiency of hydrophilic drugs. *Curr Nanosci*. 2013;9(2):211-20. doi: [10.2174/1573413711309020008](https://doi.org/10.2174/1573413711309020008).
40. Montenegro L, Sarpietro MG, Ottimo S, Puglisi G, Castelli F. Differential scanning calorimetry studies on sunscreen loaded solid lipid nanoparticles prepared by the phase inversion temperature method. *Int J Pharm*. 2011;415(1-2):301-6. doi: [10.1016/j.ijpharm.2011.05.076](https://doi.org/10.1016/j.ijpharm.2011.05.076), PMID [21679757](https://pubmed.ncbi.nlm.nih.gov/21679757/).
41. Shah M, Agrawal YK, Garala K, Ramkishan A. Solid lipid nanoparticles of a water-soluble drug ciprofloxacin hydrochloride. *Indian J Pharm Sci*. 2012;74(5):434-42. doi: [10.4103/0250-474X.108419](https://doi.org/10.4103/0250-474X.108419), PMID [23716872](https://pubmed.ncbi.nlm.nih.gov/23716872/).
42. Shen J, Burgess DJ. *In vitro* dissolution testing strategies for nanoparticulate drug delivery systems: recent developments and challenges. *Drug Deliv Transl Res*. 2013;3(5):409-15. doi: [10.1007/s13346-013-0129-z](https://doi.org/10.1007/s13346-013-0129-z), PMID [24069580](https://pubmed.ncbi.nlm.nih.gov/24069580/).
43. Uner M. Characterization and imaging of solid lipid nanoparticles and nanostructured lipid carriers. In: *Aliofkhazraei M, editor. Handbook of nanoparticles*. Berlin: Springer International Publishing; 2016. p. 117-41.
44. Kumar S, Randhawa JK. Preparation and characterization of paliperidone loaded solid lipid nanoparticles. *Colloids Surf B Biointerfaces*. 2013;102:562-8. doi: [10.1016/j.colsurfb.2012.08.052](https://doi.org/10.1016/j.colsurfb.2012.08.052), PMID [23104026](https://pubmed.ncbi.nlm.nih.gov/23104026/).
45. Madkhali OA. Perspectives and prospective on solid lipid nanoparticles as drug delivery systems. *Molecules*. 2022 Feb;27(5):1543. doi: [10.3390/molecules27051543](https://doi.org/10.3390/molecules27051543), PMID [35268643](https://pubmed.ncbi.nlm.nih.gov/35268643/).
46. Satapathy MK, Yen TL, Jan JS, Tang RD, Wang JY, Taliyan R. Solid lipid nanoparticles (SLNs): an advanced drug delivery system targeting brain through BBB. *Pharmaceutics*. 2021;13(8):1183. doi: [10.3390/pharmaceutics13081183](https://doi.org/10.3390/pharmaceutics13081183), PMID [34452143](https://pubmed.ncbi.nlm.nih.gov/34452143/).

47. Ekambaram P, Abdul HS. Formulation and evaluation of solid lipid nanoparticles of ramipril. *J Young Pharm.* 2011;3(3):216-20. doi: [10.4103/0975-1483.83765](https://doi.org/10.4103/0975-1483.83765), PMID [21897661](https://pubmed.ncbi.nlm.nih.gov/21897661/).
48. Ghadiri M, Fatemi S, Vatanara A, Doroud D, Najafabadi AR, Darabi M. Loading hydrophilic drug in solid lipid media as nanoparticles: statistical modeling of entrapment efficiency and particle size. *Int J Pharm.* 2012;424(1-2):128-37. doi: [10.1016/j.ijpharm.2011.12.037](https://doi.org/10.1016/j.ijpharm.2011.12.037), PMID [22227603](https://pubmed.ncbi.nlm.nih.gov/22227603/).
49. Awasthi R, Bhushan B, Kulkarni GT. Targeting chronic inflammatory lung diseases using advanced drug delivery systems. Amsterdam: Elsevier; 2020. p. 171-209.
50. Shah M, Pathak K. Development and statistical optimization of solid lipid nanoparticles of simvastatin by using 2³ full factorial design. *AAPS Pharm Sci Tech.* 2010;11(2):489-96. doi: [10.1208/s12249-010-9414-z](https://doi.org/10.1208/s12249-010-9414-z), PMID [20309652](https://pubmed.ncbi.nlm.nih.gov/20309652/).
51. Trotta M, Debernardi F, Caputo O. Preparation of solid lipid nanoparticles by a solvent emulsification diffusion technique. *Int J Pharm.* 2003;257(1-2):153-60. doi: [10.1016/s0378-5173\(03\)00135-2](https://doi.org/10.1016/s0378-5173(03)00135-2), PMID [12711170](https://pubmed.ncbi.nlm.nih.gov/12711170/).
52. Wang N, Hsu C, Zhu L, Tseng S, Hsu JP. Influence of metal oxide nanoparticles concentration on their zeta potential. *J Colloid Interface Sci.* 2013 Oct 1;407:22-8. doi: [10.1016/j.jcis.2013.05.058](https://doi.org/10.1016/j.jcis.2013.05.058), PMID [23838331](https://pubmed.ncbi.nlm.nih.gov/23838331/).
53. Akbari B, Tavandashti MP, Zandrahimi M. Particle size characterization of nanoparticles a practical approach. *Iran J Mater Sci Eng.* 2011;8(2):48-56.
54. Apostolou M, Assi S, Fatokun AA, Khan I. The effects of solid and liquid lipids on the physicochemical properties of nanostructured lipid carriers. *J Pharm Sci.* 2021;110(8):2859-72. doi: [10.1016/j.xphs.2021.04.012](https://doi.org/10.1016/j.xphs.2021.04.012), PMID [33901564](https://pubmed.ncbi.nlm.nih.gov/33901564/).
55. Dhoranwala KA, Shah P, Shah S. Formulation optimization of rosuvastatin calcium loaded solid lipid nanoparticles by 3² full factorial designs. *Nanoworld J.* 2015;1(4):112-21. doi: [10.17756/nwj.2015-015](https://doi.org/10.17756/nwj.2015-015).
56. Zambaux MF, Bonneaux F, Gref R, Maincent P, Dellacherie E, Alonso MJ. Influence of experimental parameters on the characteristics of poly (lactic acid) nanoparticles prepared by a double emulsion method. *J Control Release.* 1998;50(1-3):31-40. doi: [10.1016/s0168-3659\(97\)00106-5](https://doi.org/10.1016/s0168-3659(97)00106-5), PMID [9685870](https://pubmed.ncbi.nlm.nih.gov/9685870/).
57. Reddy KR, Satyanarayana SV, Reddy VJ. Development and evaluation of clobetasol-loaded solid lipid nanoparticles for topical treatment of psoriasis. *Int J App Pharm.* 2019;11(5):143-50. doi: [10.22159/ijap.2019v11i5.33592](https://doi.org/10.22159/ijap.2019v11i5.33592).
58. Alshora DH, Ibrahim MA, Elzayat E, Almeanazel OT, Alanazi F. Rosuvastatin calcium nanoparticles: improving bioavailability by formulation and stabilization codesign. *Plos One.* 2018;13(7):e0200218. doi: [10.1371/journal.pone.0200218](https://doi.org/10.1371/journal.pone.0200218), PMID [29985967](https://pubmed.ncbi.nlm.nih.gov/29985967/).
59. Danaei M, Dehghankhold M, Ataei S, Hasanzadeh Davarani F, Javanmard R, Dokhani A. Impact of particle size and polydispersity index on the clinical applications of lipidic nanocarrier systems. *Pharmaceutics.* 2018;10(2):57. doi: [10.3390/pharmaceutics10020057](https://doi.org/10.3390/pharmaceutics10020057), PMID [29783687](https://pubmed.ncbi.nlm.nih.gov/29783687/).
60. Akanda M, Mithu MS, Douroumis D. Solid lipid nanoparticles: an effective lipid-based technology for cancer treatment. *Journal of Drug Delivery Science and Technology.* 2023 Sep;86:104709. doi: [10.1016/j.jddst.2023.104709](https://doi.org/10.1016/j.jddst.2023.104709).
61. Schubert MA, Muller Goymann CC. Solvent injection as a new approach for manufacturing lipid nanoparticles evaluation of the method and process parameters. *Eur J Pharm Biopharm.* 2003;55(1):125-31. doi: [10.1016/s0939-6411\(02\)00130-3](https://doi.org/10.1016/s0939-6411(02)00130-3), PMID [12551713](https://pubmed.ncbi.nlm.nih.gov/12551713/).
62. Kesharwani R, Sachan A, Singh S, Patel D. Formulation and evaluation of solid lipid nanoparticle (SLN) based topical gel of etoricoxib. *J App Pharm Sci.* 2016;6(10):124-31. doi: [10.7324/JAPS.2016.601017](https://doi.org/10.7324/JAPS.2016.601017).
63. Qushawy M, Nasr A. Solid lipid nanoparticles (SLNs) as nano drug delivery carriers: preparation characterization and application. *Int J App Pharm.* 2019;12(1):1-9. doi: [10.22159/ijap.2020v12i1.35312](https://doi.org/10.22159/ijap.2020v12i1.35312).
64. Dudhipala N, Veerabrahma K. Improved anti-hyperlipidemic activity of rosuvastatin calcium via lipid nanoparticles: pharmacokinetic and pharmacodynamic evaluation. *Eur J Pharm Biopharm.* 2017 Jan;110:47-57. doi: [10.1016/j.ejpb.2016.10.022](https://doi.org/10.1016/j.ejpb.2016.10.022), PMID [27810472](https://pubmed.ncbi.nlm.nih.gov/27810472/).
65. Hunter RJ. Zeta potential in colloid science: principles and applications volume 2 of colloid science colloid science. A series of monographs volume 2 of human communication research series 385; 1981.
66. Blanco E, Shen H, Ferrari M. Principles of nanoparticle design for overcoming biological barriers to drug delivery. *Nat Biotechnol.* 2015 Sep;33(9):941-51. doi: [10.1038/nbt.3330](https://doi.org/10.1038/nbt.3330), PMID [26348965](https://pubmed.ncbi.nlm.nih.gov/26348965/).
67. Dhoranwala KA, Shah P, Shah S. Formulation optimization of rosuvastatin calcium loaded solid lipid nanoparticles by 3² full factorial design. *Nanoworld J.* 2015;1(4):112-21. doi: [10.17756/nwj.2015-015](https://doi.org/10.17756/nwj.2015-015).
68. Duong VA, Nguyen TT, Maeng HJ. Preparation of solid lipid nanoparticles and nanostructured lipid carriers for drug delivery and the effects of preparation parameters of solvent injection method. *Molecules.* 2020 Oct 18;25(20):4781. doi: [10.3390/molecules25204781](https://doi.org/10.3390/molecules25204781), PMID [33081021](https://pubmed.ncbi.nlm.nih.gov/33081021/).
69. Kishore CR, Mohan GV. Structural identification and estimation of rosuvastatin calcium-related impurities in rosuvastatin calcium tablet dosage form. *Anal Chem Res.* 2017;12:17-27. doi: [10.1016/j.ancr.2016.11.002](https://doi.org/10.1016/j.ancr.2016.11.002).
70. Jores K, Mehnert W, Drechsler M, Bunjes H, Johann C, Mader K. Investigations on the structure of solid lipid nanoparticles (SLN) and oil loaded solid lipid nanoparticles by photon correlation spectroscopy field flow fractionation and transmission electron microscopy. *J Control Release.* 2004 Mar 5;95(2):217-27. doi: [10.1016/j.jconrel.2003.11.012](https://doi.org/10.1016/j.jconrel.2003.11.012), PMID [14980770](https://pubmed.ncbi.nlm.nih.gov/14980770/).